
GRAPH SPRING NEURAL ODES FOR LINK SIGN PREDICTION

Andrin Rehmann

Pasteur Labs
New York
USA
andrinrehmann@gmail.com

Alexandre Bovet

Department of Mathematical Modeling and Machine Learning
Digital Society Initiative
University of Zurich
Switzerland
alexandre.bovet@uzh.ch

December 18, 2024

ABSTRACT

Signed graphs allow for encoding positive and negative relations between nodes and are used to model various online activities. Node representation learning for signed graphs is a well-studied task with important applications such as sign prediction. While the size of datasets is ever-increasing, recent methods often sacrifice scalability for accuracy. We propose a novel message-passing layer architecture called Graph Spring Network (GSN) modeled after spring forces. We combine it with a Graph Neural Ordinary Differential Equations (ODEs) formalism to optimize the system dynamics in embedding space to solve a downstream prediction task. Once the dynamics is learned, embedding generation for novel datasets is done by solving the ODEs in time using a numerical integration scheme. Our GSN layer leverages the fast-to-compute edge vector directions and learnable scalar functions that only depend on nodes' distances in latent space to compute the nodes' positions. Conversely, Graph Convolution and Graph Attention Network layers rely on learnable vector functions that require the full positions of input nodes in latent space. We propose a specific implementation called Spring-Neural-Network (SPR-NN) using a set of small neural networks mimicking attracting and repulsing spring forces that we train for link sign prediction. Experiments show that our method achieves accuracy close to the state-of-the-art methods with node generation time speedup factors of up to 28,000 on large graphs.

Keywords Graph machine learning, Signed Graphs, Node Representation Learning, Sign Prediction, Graph Neural Ordinary Differential Equations

1 Introduction

Signed graphs distinguish negative and positive edges, also called link signs. They are crucial to modeling relations in online platforms, such as attitudes between users in social media or preferences between users and products in online stores. The ability to predict new links and their type - either negative or positive - between users is crucial for analyzing and understanding dynamics in social networks [Leskovec et al., 2010] or for improving recommender systems [Huang et al., 2023].

Methods for link sign prediction often involve social balance theory [Cartwright and Harary, 1956], which postulates that triangles in a network, where edges represent attitudes or relations of liking, tend to be balanced, i.e., the product of the signs of three edges in a triad is positive. However, not all triadic relationships in real-world networks satisfy this rule, and some edges do not participate in a triad. Hence, reliable predictions require extending or replacing rule-based approaches with heuristic models. Typically, the problem is solved in a two-step procedure. First, a multidimensional vector, or node embedding, is generated for all nodes based on the available edge signs and graph structure. Subsequently, the Euclidean distance between the node embeddings of adjacent nodes serves as an input to a logistic regression model, which is then used to infer the signs of the edges [Huang et al., 2021, Derr et al., 2018]. The embedding vectors are frequently generated using a graph neural network (GNN), which iteratively improves the embedding through training. Often, a term capturing social balance theory is included in the loss function. Although

architecture designs vary across different methods, the overall framework remains similar. The approach offers high inference accuracy; however, the process does not scale well for large graphs.

In this work, we generate the embeddings from the time-evolved states obtained by solving second-order ordinary differential equations (ODEs) involving the nodes’ positions. To this end, each node is associated with a vector position in the embedding space, which is initially random. By cleverly designing a function for the 2nd-order time derivative of the node positions, the system evolves forward in time, leading to final node positions that can be leveraged to solve the downstream link sign prediction task. We model the dynamics of the second-order ODEs with two learnable scalar functions. The first scalar function is evaluated on each edge and reads edge and adjacent node attributes. Its resulting value is then used to scale the direction vector associated with the edge in latent space, resulting in an edge force vector. Those vectors are then summed up and scaled with the second learnable function, constituting the position vector’s second-order derivative in latent space. The ODEs system is then solved with a numerical integrator, whereas the final node positions in latent space are taken as the node embeddings. The continuous modeling approach using learnable functions to model the time derivative of a system’s state corresponds to the framework of Graph Neural ODE’s [Poli et al., 2019, Rusch et al., 2022, Sun et al., 2024]. Whereas previous research leveraged common neighborhood coupling functions such as Graph Convolutional Networks (GCN) or Graph Attention Networks (GAT), we propose a novel message-passing layer architecture termed Graph Spring Network (GSN). In contrast to GCN or GAT, the number of learnable parameters of the GSN layer is independent of the number of dimensions of the latent space. Subsequently, the computational time of inference and training is lower due to the reduced parameter count. In contrast to discrete modeling approaches used to solve link sign prediction task [Liu, 2022, Huang et al., 2021, Li et al., 2020, Islam et al., 2018, Ren et al., 2024, Chung and Whang, 2023], the continuous modeling approach allows us to learn the dynamics of the ODE once, and generate node embeddings on unseen datasets without training. This can be done because the solution is found by solving the ODEs with a numerical solver, which gives our approach good generalization properties.

We propose two distinct approaches to model the GSN layer, Spring (SPR) and Spring Neural Network (SPR-NN). SPR is based on Hooke’s law - an equation to model the dynamics in physical springs and SPR-NN leverages a small, shallow artificial neural network. The constants specifying the dynamics of spring equations in SPR and the neural network parameters in SPR-NN are optimized using a gradient-based optimization method. Both methods achieve competitive accuracy scores across all examined datasets, where SPR-NN is significantly more accurate than SPR. At the same time, our method demonstrates runtime improvements by a factor 10^5 for large graphs compared to a methods with similar accuracy. The main contributions of this paper are as follows:

- We propose a novel message passing architecture, Graph Spring Network (GSN), for scalable node embedding generation and derive its computational complexity.
- We propose two novel methods for link sign prediction, Spring (SPR) and Spring Neural Network (SPR-NN), based on GSN.
- We demonstrate their effectiveness and performance on real-world signed graphs, showing that SPR-NN achieves comparable accuracy to state-of-the-art methods while outperforming them in terms of runtime.

2 Related Work

2.1 Link Sign Prediction with Discrete Modeling

In discrete modeling approaches, a neural network with a fixed number of layers is used to predict the next state of interest of the inference. The first methods proposed for sign inference in signed graphs are based on formulating rules-based extensions of the structural balance theory [Guha et al., 2004, Song and Meyer, 2015]. Leskovec et al. [2009] proposed a logistic regression trained on several extracted node features, such as degrees and the number of incoming negative and positive edges. Advancements in machine learning and increased computing powers enabled graph embedding generation approaches, pioneered by Deepwalk [Perozzi et al., 2014] and Node2Vec [Grover and Leskovec, 2016]. Both methods train and generate node embedding using stochastic gradient descent. The node vectors are generated so that spatial proximity in the embedding space correlates with proximity on the structural level in the graph. However, these approaches target link prediction for unsigned networks. Later methods were explicitly designed for link sign prediction [Chung and Whang, 2023, Ren et al., 2024, Shi et al., 2024]. For example, Wang et al. [2017] introduced *SiNE*, an embedding generation method integrating social balance theory for link sign prediction in social media. Signed Graph Convolutional Networks (*SGCN*) is the first method to apply a graph convolutional network architecture specifically to undirected link sign prediction [Derr et al., 2018]. The approach has been refined with *LightSGCN* [Liu, 2022]. Graph Convolutional Network architectures for directed link sign prediction were also proposed with *BRIDGE* [Chen et al., 2018a], *SIGNET* [Islam et al., 2018], *SDGNN* [Huang et al., 2021] and *SELO* [Fang et al., 2023]. The attention mechanism was introduced to graph neural networks [Veličković et al., 2017], which

was then adapted to signed networks by Huang et al. [2019] with *SiGAT* and refined and improved in follow-up work [Li et al., 2020, Shi et al., 2024]. A spectral graph theory and graph signal processing approach was also recently proposed by Li et al. [2023] with *SLGNN*. Other recent developments in the field include the study of adversarial attacks against link prediction in signed networks [Lizurej et al., 2023, Lee et al., 2024] and link sign prediction in multilayer signed graphs [Ren et al., 2024].

2.2 Continuous Modeling for Node Representation Learning

In contrast to discrete modeling approaches, continuous modeling approaches learn the temporal dynamics of a system. Learning with continuous systems can be more memory efficient and less prone to over-smoothing when information propagation across a large graph is crucial [Xhonneux et al., 2020]. Chen et al. [2018b] introduced the Neural ODEs framework as a family of continuous-depth models where the dynamics of ODEs is learned by modeling the first-order derivative of the state using an artificial neural network. The Graph Neural ODEs framework, extending Neural ODEs to graph-structured datasets, proposed by Poli et al. [2019] defines the derivatives of nodes’ representations as a combination of the current node representations, the representations of neighbors, and the initial values of the nodes. The approach was extended with a self-attention mechanism and an encoder network [Huang et al., 2020]. With *GraphCon* [Rusch et al., 2022], the Graph Neural ODE framework was extended by learning the second instead of first-order ODEs dynamics and adding a damping term for stability. Independently Sanchez-Gonzalez et al. [2019] proposed a GNN approach with learnable ODEs based on a Hamiltonian mechanics formalism, which was later extended by Kang et al. [Kang et al., 2023]. The Graph Neural ODE-based approach has recently been applied to link sign prediction in dynamic graphs with DynamicSE [Sun et al., 2024]. Graph Neural ODEs also take inspiration from diffusion processes on graphs, such as random walks [Xhonneux et al., 2020, Chamberlain et al., 2021]. Signed graph diffusion approaches have also been applied to generate node representations of signed graphs [Jung et al., 2020, Choi et al., 2023] and for link sign prediction with *SDGNet* [Jung et al., 2020].

2.3 Force Directed Graph Algorithms

Force-directed approaches model nodes as particles and evolve their positions forward in time with a numerical solver. Typically, they do it in two dimensions to visualize the final node positions with a scatter plot. Fruchterman and Reingold [1991] proposed attracting spring forces between adjacent nodes and repulsing electrical force between all nodes. The combination ensures the closeness of connected nodes while retaining visual distinctiveness between nodes. This principle has been iteratively improved in follow-up work [Kamada et al., 1989, Hadany and Harel, 2001]. Moving beyond visualization, force-directed approaches have also been applied to link prediction tasks [Rahman et al., 2020, Lotfalizadeh and Al Hasan, 2023], which can be done by increasing the embedding dimension and interpreting the node positions as node embeddings.

3 Background

3.1 Problem Statement

We consider a signed undirected graph $G = (V, E, \sigma)$, with V representing the set of nodes and E denoting the set of edges and the function $\sigma : V \times V \rightarrow \{-1, 1\}$ assigning a sign of either -1 or 1 to each edge $(i, j) \in E$. The total number of nodes in the graph is expressed as $|V| = N$. We derive a secondary graph G' from the original graph G to evaluate our prediction method. In G' , a specified percentage p_{hidden} of edge signs is obscured. The altered graph is defined as $G' = (V, E, \sigma')$, where V and E remain unchanged, while $\sigma' : V \times V \rightarrow \{-1, 0, 1\}$ is designed as

$$\sigma'(i, j) = \begin{cases} \sigma(i, j) & \text{if } \mathbb{P}(Y > p_{\text{hidden}}) \\ 0 & \text{otherwise,} \end{cases} \quad (1)$$

where Y is a random variable with a uniform distribution between 0 and 1 and \mathbb{P} denotes the probability function. We aim to infer a sign prediction function $\hat{\sigma} : V \times V \rightarrow \{-1, 1\}$, capable of approximating the original sign function σ as closely as possible. Note that our approach allows us to set neutral values to the edges whose sign we wish to infer. Our problem formulation differs from other formulations where edges in the test set are completely removed from the graph instead of marking them as neutral.

4 Framework

4.1 Graph Spring Network Layer

Without any loss of generality, a message passing layer can be defined as [Bronstein et al., 2021]

$$\text{mpl}(\mathbf{x}_i) = \phi \left(\mathbf{y}_i, \mathbf{x}_i \bigoplus_{j \in N_i} \psi(\mathbf{x}_i, \mathbf{x}_j, \mathbf{z}_{i,j}) \right), \quad (2)$$

where N_i denotes the set of neighboring nodes of i , $\mathbf{z}_{i,j}$ and \mathbf{y}_i the static edge and node features, \bigoplus is an aggregation operations, ϕ and ψ differentiable functions and $\mathbf{x}_i \in \mathbb{R}^k$ the dynamic node representations. We define a specific message-passing layer called Graph Spring Network (GSN) as

$$\text{gsn}(\mathbf{x}_i) = g(\mathbf{y}_i) \cdot \sum_{j \in N_i} f(\mathbf{z}_{i,j}, d(\mathbf{x}_i, \mathbf{x}_j)) \cdot \frac{\mathbf{x}_j - \mathbf{x}_i}{d(\mathbf{x}_i, \mathbf{x}_j)} \quad (3)$$

where d denotes the Euclidean distance between two nodes

$$d(\mathbf{x}_i, \mathbf{x}_j) = \sqrt{(\mathbf{x}_i - \mathbf{x}_j)^2} \quad (4)$$

and f, g are differentiable scalar functions, which could be functions with learnable parameters such as a neural network. The node features, \mathbf{y}_i , and edge features, \mathbf{z}_i , are both independent of the node positions in the embedding space. In contrast to other layers, such as a GCN or GAT, which use learnable vector functions with the full nodes' positions as input, the learnable scalar functions involved with GSN only read the distance vectors between adjacent nodes and static graph features. Hence, the complexity of the learnable functions can be greatly reduced as the number of data processed is significantly lower. As detailed in section 4.4, we can construct two scalar functions that rely on a total of seven learnable parameters and still solve a downstream prediction task using the GSN layer.

4.2 Graph Spring Network Layer Complexity

We denote the size of the embedding space as k , N as the number of nodes, and M as the number of edges. The time complexity of a single graph convolution or a graph attention layer is $Mk + Nk^2$ [Blakely et al., 2021]. We analyze the complexity of the GSN layer by decomposing Equation 3 into three operations

1. Edge level transformation:

$$\mathbf{a}_{i,j} = f(\mathbf{z}_{i,j}, d(\mathbf{x}_i, \mathbf{x}_j)) \cdot \frac{\mathbf{x}_j - \mathbf{x}_i}{d(\mathbf{x}_i, \mathbf{x}_j)}. \quad (5)$$

2. Neighborhood aggregation:

$$\mathbf{b}_i = \sum_{j \in N_i} \mathbf{a}_{i,j}. \quad (6)$$

3. Node level transformation:

$$g(\mathbf{y}_i) \cdot \mathbf{b}_i. \quad (7)$$

Part 1 is made of a vector subtraction ($O(k)$), a computation of a vector distance ($O(1)$), and an evaluation of the function f which is independent of k ($O(1)$). Part 1 is done for all edges; hence, its complexity is $O(Mk)$. Part 2 is a summation of the k dimensional vectors resulting from part 1. The operation is done for the average number of degrees ($O(\frac{M}{N}k)$), which is repeated for all nodes; hence its complexity is $O(N\frac{M}{N}k + Nk) = O(Mk + Nk)$. Part 3 is a vector scaling repeated for all nodes resulting in $O(Nk)$. Adding all parts together yields $O(Mk + Mk + Nk + Nk) = O(Mk + Nk)$.

4.3 Temporal Dynamics

We use a single GSN layer in combination with Graph Neural Ordinary Differential Equations [Poli et al., 2019], obtaining the initial-value problem defined by

$$\frac{d\mathbf{v}_i(t)}{dt} = \text{gsn}(\mathbf{x}_i(t)), \quad (8)$$

$$\frac{d\mathbf{x}_i(t)}{dt} = \mathbf{v}_i, \quad (9)$$

$$\mathbf{x}_i(0) \sim \mathcal{U}_{(-1,1)} \quad (10)$$

and

$$\mathbf{v}_i(t) = 0. \quad (11)$$

which can be solved using any numerical ODE solver. Here \mathbf{v}_i denotes the velocity of node i and $\mathcal{U}_{(-1,1)}$ the random uniform distribution on $(-1, 1)$.

4.4 SPR: Spring Based Forces

The central premise of our approach is that by customizing the scalar functions f and g and choosing appropriate parameters, we can influence the lengths of edges with unknown signs to either expand or contract to an appropriate length with respect to their surrounding. To this end, our first method uses an adapted version of Hooke’s law, which describes the physical forces in a spring. A spring exerts a force linearly proportional to the difference between its resting length and actual length. For each edge type, positive, neutral, and negative, we assign distinct resting lengths: l^+ for positive, l^\pm for neutral, and l^- for negative edges. Accompanying these resting lengths are the respective stiffness coefficients, α^+ for positive, α^\pm for neutral, and α^- for negative interactions, with all coefficients being real-valued parameters. We organize all learnable parameters in a vector θ . The scalar function f is defined as

$$f(\theta_f, \mathbf{z}_{ij}) = \begin{cases} \alpha^\mp \cdot (d(\mathbf{x}_j, \mathbf{x}_i) - l^\mp) & \text{if } \sigma'(i, j) \text{ is } 0 \\ \alpha^+ \cdot \max(d(\mathbf{x}_j, \mathbf{x}_i) - l^+, 0) & \text{if } \sigma'(i, j) \text{ is } 1 \\ -\alpha^- \cdot \max(l^- - d(\mathbf{x}_j, \mathbf{x}_i), 0) & \text{if } \sigma'(i, j) \text{ is } -1 \end{cases} \quad (12)$$

where

$$\mathbf{z}_{ij} = [d(\mathbf{x}_i, \mathbf{x}_j)] \quad (13)$$

and

$$\theta_f = [l^+ \quad l^\mp \quad l^- \quad \alpha^+ \quad \alpha^\mp \quad \alpha^-]^\top. \quad (14)$$

In the case of $\sigma'(i, j) = 0$, equation 12 directly follows Hooke’s law. If the edge is negative ($\sigma'(i, j) = -1$), we apply a force that pushes the adjacent nodes apart from each other. If two nodes lie at a distance greater than l^- no force is applied, hence they can freely drift apart from each other. Analogously, for positive edges ($\sigma'(i, j) = 1$), we apply an attraction force between connected nodes only when they are farther apart than l^+ . If they are closer, no forces are applied. We define function g as

$$g(\beta, \mathbf{y}_i) = (\min(1, \text{deg}_i / p_{80}) \cdot \beta + 1) \quad (15)$$

where

$$\mathbf{y}_i = [\text{deg}_i, p_{80}]. \quad (16)$$

The function g ensures stronger forces for nodes with a higher connectivity. The term p_{80} represents the 80th percentile of the graph’s degree distribution. The scaling term maps the node degrees to a range between 0 and 1 and caps it at the 80-th percentile. The learnable variable β controls the strength of this scaling factor. We have modeled g (15) based on observations showing that the number of correctly predicted edge signs adjacent to a node correlates with the node degree. All the learnable parameters from SPR are organized in the vector

$$\theta_{spring} = [\theta_f \quad \beta]^\top. \quad (17)$$

4.5 SPR-NN: Neural Network Based Forces

In our second approach, we model f based on the structure of a multi-layer perception (MLP). We define a shallow MLP with a single hidden layer as

$$\text{MLP}(\theta_{\text{MLP}}, \mathbf{z}_{ij}) = \mathbf{W}_1 \times \text{ReLU}(\mathbf{W}_0 \times \mathbf{z}_{ij} + \mathbf{b}_0) + \mathbf{b}_1 \quad (18)$$

where \mathbf{W}_0 , \mathbf{W}_1 , \mathbf{b}_0 and \mathbf{b}_1 are weight matrices and respectively bias vectors of the MLP. \mathbf{z}_{ij} denotes a static edge feature vector, and ReLU denotes a rectified linear unit activation function. Finally

$$\theta_{\text{MLP}} = [\mathbf{W}_0 \quad \mathbf{W}_1 \quad \mathbf{b}_0 \quad \mathbf{b}_1]^\top. \quad (19)$$

The function f is made of three equivalent but individually parameterized neural networks

$$f(\theta_f, \mathbf{z}_{ij}) = \begin{cases} \text{MLP}(\theta_0, \mathbf{z}_{ij}) & \text{if } \sigma'(i, j) \text{ is } 0 \\ \text{MLP}(\theta_1, \mathbf{z}_{ij}) & \text{if } \sigma'(i, j) \text{ is } 1 \\ \text{MLP}(\theta_2, \mathbf{z}_{ij}) & \text{if } \sigma'(i, j) \text{ is } -1 \end{cases}, \quad (20)$$

where

$$\theta_f = [\theta_0 \quad \theta_1 \quad \theta_2]^\top. \quad (21)$$

The size of the hidden layer for each MLP is seven, hence $\mathbf{W}_0 \in \mathbb{R}^{7 \times 7}$, $\mathbf{W}_1 \in \mathbb{R}^7$, $\mathbf{b}_0 \in \mathbb{R}^7$, $\mathbf{b}_1 \in \mathbb{R}$. The edge specific input vector \mathbf{z}_{ij} is defined as

$$\mathbf{z}_{ij} = [d(\mathbf{x}_i, \mathbf{x}_j) \quad \text{deg}_i \quad \text{deg}_j \quad \text{neg}_i \quad \text{neg}_j \quad \text{pos}_i \quad \text{pos}_j]^\top. \quad (22)$$

The variables neg_i and pos_i represent the fractions of negative and positive edges connected to node i . Given that some edges are unknown during training, neg_i and pos_i are crucial for our analysis. Naturally, the features are constructed without knowing the true sign distribution function σ .

The function g is

$$g(\theta_g, \mathbf{z}_i) = \text{MLP}(\theta_g, \mathbf{z}_i) \quad (23)$$

with $\mathbf{W}_0 \in \mathbb{R}^{3 \times 3}$, $\mathbf{W}_1 \in \mathbb{R}^3$, $\mathbf{b}_0 \in \mathbb{R}^3$, $\mathbf{b}_1 \in \mathbb{R}$. Hence the complete parameter vector

$$\theta_{nn} = [\theta_g \quad \theta_f]^\top \quad (24)$$

contains 8 weight matrices and 8 bias vectors, totalling in 184 parameters.

5 Simulation and Training

The second-order ODE of the embedding vector \mathbf{x} is equivalent to the equation of motion with a constant mass of one. Hence, acceleration is equal to force and

$$\frac{d^2 \mathbf{x}_i}{dt^2} = \frac{d\mathbf{v}_i}{dt} = \mathbf{f}_i, \quad (25)$$

which can be solved by the Euler method. In this section, we describe the forward simulation and the optimization process, which leverages a differentiable formulation of the forward simulation to learn θ_{spring} and θ_{nn} .

5.1 Forward Simulation

We introduce the time-dependent position, velocity and force tensors

$$\mathbf{X}(t) = \begin{bmatrix} \mathbf{x}_0^\top(t) \\ \mathbf{x}_1^\top(t) \\ \vdots \\ \mathbf{x}_N^\top(t) \end{bmatrix} \in \mathbb{R}^{N \times k}, \quad \mathbf{V}(t) = \begin{bmatrix} \mathbf{v}_0^\top(t) \\ \mathbf{v}_1^\top(t) \\ \vdots \\ \mathbf{v}_N^\top(t) \end{bmatrix} \in \mathbb{R}^{N \times k} \quad (26)$$

$$\text{and } \mathbf{F}(t) = \begin{bmatrix} \mathbf{f}_0^\top(t) \\ \mathbf{f}_1^\top(t) \\ \vdots \\ \mathbf{f}_N^\top(t) \end{bmatrix} \in \mathbb{R}^{N \times k}. \quad (27)$$

The functions f and g of the forces \mathbf{f} can be either chosen as defined for SPR or SPR-NN. The equations to advance $\mathbf{V}(t)$ and $\mathbf{X}(t)$ in time are

$$\mathbf{V}(t + dt) = (1 - d) \cdot \mathbf{V}(t) + dt \cdot \mathbf{F}(t) \quad (28)$$

and

$$\mathbf{X}(t + dt) = \mathbf{X}(t) + dt \cdot \mathbf{V}(t), \quad (29)$$

where d is a linear damping factor, which increases the numerical stability. Using the state vector notation $\mathbf{S}(t) = [\mathbf{X}(t) \mathbf{V}(t)]^\top$, we define the update function Φ which advances the state by a time step dt as

$$\Phi(\mathbf{S}(t)) = \begin{bmatrix} 1 & 0 \\ 0 & (1 - d) \end{bmatrix} \mathbf{S}(t) + dt \begin{bmatrix} \mathbf{V}(t) \\ \mathbf{F}(t) \end{bmatrix}. \quad (30)$$

Hence a forward simulation is a composition of Φ functions

$$\mathbf{S}(n) = \overbrace{(\Phi \circ \dots \circ \Phi)}^{n\text{-times}}(\mathbf{S}(0)) \quad (31)$$

where n denotes the number of simulation steps. The initial state of the system, $\mathbf{S}(0)$, is defined as described in equations 10 and 11. The time complexity of the entire forward simulation is $O(n(Nk + Mk))$ as it is a chain of GSN layers, each with a complexity of $O(Nk + Mk)$.

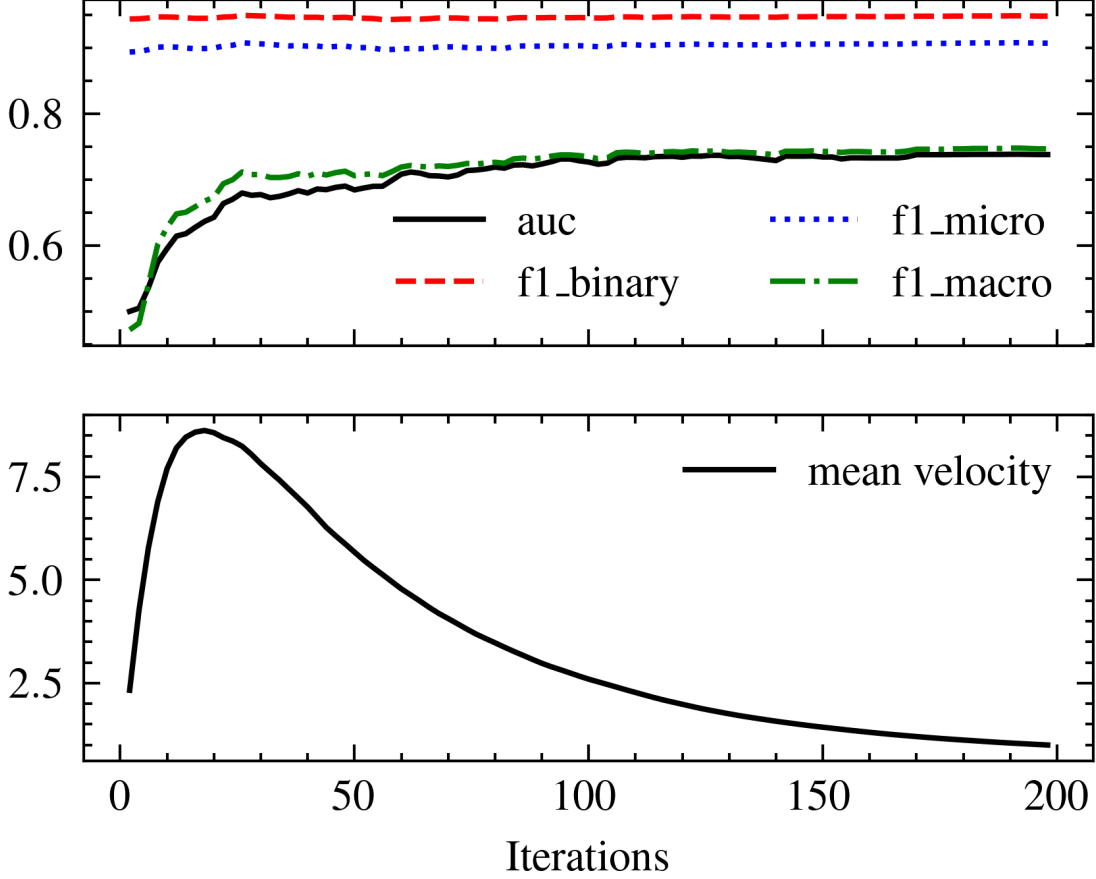


Figure 1: Forward simulation of SPR-NN on BitcoinAlpha. The mean velocity is equivalent to $\frac{dx}{dt}$.

5.2 Parameter Learning

To learn parameters θ_{spring} and θ_{nn} , we leverage a gradient based optimization method, hence a differentiable loss function needs to be found. Sign prediction is a discrete task, however we can map the edge lengths to the interval $[0, 1]$ using a logistic function with a threshold μ

$$\hat{\sigma}(u, v) = \left(1 + e^{\|\mathbf{x}_u - \mathbf{x}_v\|_2 - \mu}\right)^{-1} \quad (32)$$

transforming it into a prediction task with a notion of confidence. This formulation allows us to define the loss as the weighted mean squared difference between the prediction $\hat{\sigma}$ and the ground truth σ

$$L(G, \mathbf{S}(t)) = \sum_{(u, v) \in E} (\sigma(u, v) - \hat{\sigma}(u, v))^2 \cdot \omega(u, v), \quad (33)$$

with normalization function

$$\omega(u, v) = \begin{cases} \frac{1}{|E^+|} & \text{if } \sigma'(u, v) = 1 \\ \frac{1}{|E^-|} & \text{if } \sigma'(u, v) = -1 \end{cases}, \quad (34)$$

which ensures an equal contribution of positive and negative predictions to the loss function, which is important in unbalanced datasets (see Tab. 1). Finally, the gradient of the loss function with respect to the parameters θ we wish to learn is given by

$$\nabla L = \frac{\partial L}{\partial \mathbf{S}(n)} \frac{\partial \mathbf{S}(n)}{\partial \theta} + \frac{\partial L}{\partial \theta}, \quad (35)$$

where in our case θ could be either θ_{spring} or θ_{nn} . With modern Automatic Differentiation (AD) libraries, ∇L can be obtained directly by calling a gradient computation function, with the loss function including the entire forward

simulation as a parameter. In our case, we use the JAX library [Bradbury et al., 2018]. The gradient needs to be back-propagated over the full chain of forward solver steps, leading to exploding and vanishing gradients [Thuerey et al., 2021]. To address the exploding gradients problem we clip the gradient to a range $[-1, 1]$ [Zhang et al., 2019]. We then use the Adam optimization algorithm [Kingma and Ba, 2014] to improve the parameters gradually. The decrease in loss and increase in the classification metrics AUC and F1-Macro can be observed in Figures 1 and 2. A drawback of applying AD on an iterative solver to obtain ∇L is a memory load that increases linearly with the number of forward iteration steps.

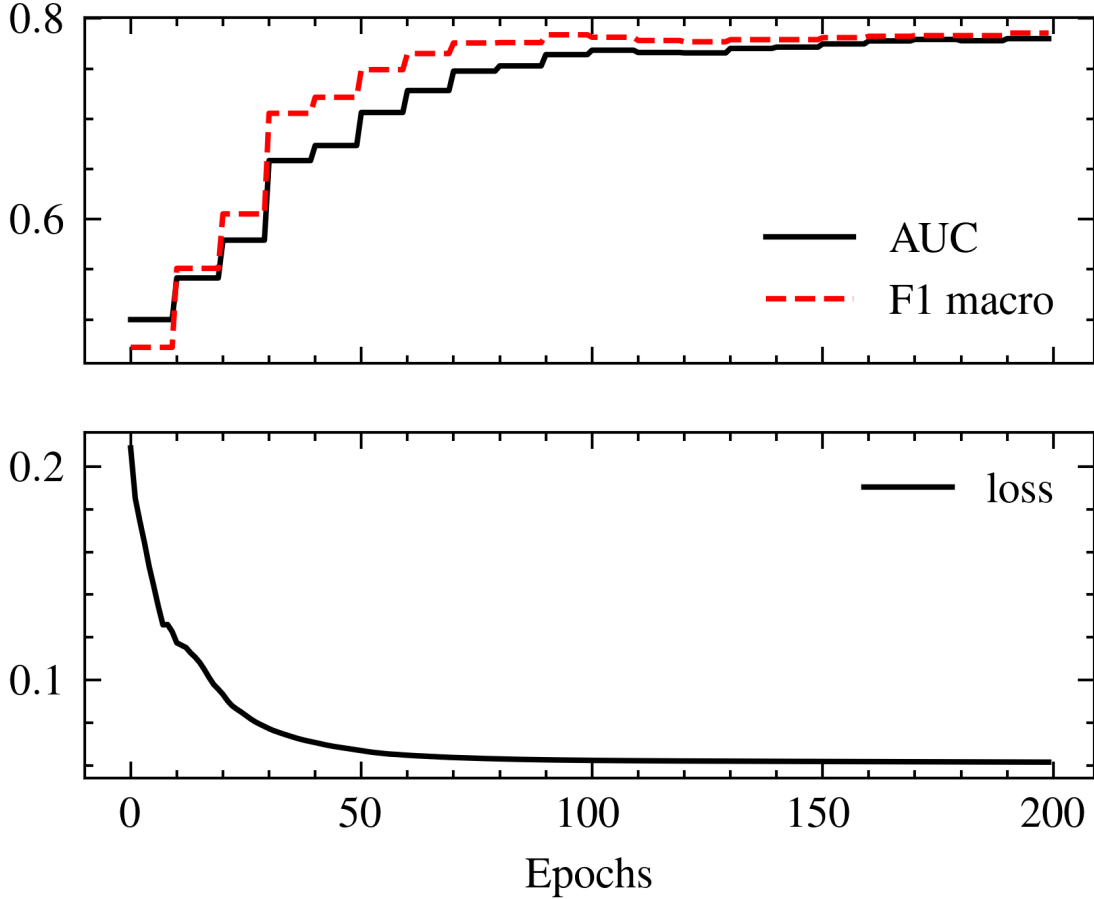


Figure 2: Training of SPR-NN on BitcoinAlpha.

6 Experiments

6.1 Datasets

We evaluate our methods on four empirical signed networks.

- BitcoinAlpha and BitcoinOTC are networks where users can indicate their level of trust for other users in integer values between -10 and 10 [Kumar et al., 2016]. We process the levels by taking the sign of the level as the sign of the edge.
- Slashdot is a platform that features user-edited content, where users can mark other users as friends or foes [Leskovec et al., 2009].
- Epinions is a social network where users can indicate their trust and distrust against other users [Richardson et al., 2003].

Table 1: Proportion of positive edges, number of edges and nodes of each network in the test datasets.

	Positive Edges	Edges M	Nodes N
Bitcoin Alpha	0.900	24186	3783
Bitcoin OTC	0.848	35592	5881
Slashdot	0.773	516575	77357
Epinions	0.829	841372	131828

The characteristics of each network are shown in Table. 1. We chose these datasets because they represent different types of signed networks, cover network sizes from small to large, and have been regularly used for comparisons by other authors. We convert directed into undirected graphs. For each edge (i, j) in the undirected graph, we add the reverse edge from (j, i) with an identical sign. If the reverse edge already exists in the dataset and there is a disagreement in sign, we prioritize the negative connection, converting both to negative as it is common practice [Wang et al., 2017, Derr et al., 2018].

6.2 Compared Methods

We compare SPR and SPR-NN with state-of-the-art methods for link sign prediction.

- SIGNET introduces a random walk method to preserve structural equilibrium in signed networks [Islam et al., 2018].
- SGCN extends the Graph Convolutional Network (GCN) framework to accommodate signed networks, drawing on balance theory principles [Derr et al., 2018].
- SiGAT integrates graph motifs specific to signed networks into the Graph Attention Network (GAT) model, leveraging balance theory and status theory [Huang et al., 2019].
- SNEA employs an attention mechanism rooted in balance theory to evaluate the importance of various neighbors during information dissemination [Li et al., 2020].
- SGDNET utilizes a random walk technique to diffuse information across the network [Jung et al., 2020].
- SDGNN offers a comprehensive approach to reconstruct the signs of links simultaneously, the directions of links, and signed directed triangles, enhancing the modeling of signed networks [Huang et al., 2021].
- SLGNN leverages spectral graph theory and graph signal processing to extract and combine low- and high-frequency information from positive and negative links. It uses a self-gating mechanism to dynamically adjust the influence of this information [Li et al., 2023].

For training SPR-NN and SPR, we use the following settings: embedding dimension $k = 64$, damping factor $d = 0.05$, temporal resolution $dt = 0.005$ and threshold $\mu = 2.5$, with a learning rate of 0.03, which we train over 200 epochs with 120 Euler integration iterations each. We have not used any hyperparameter tuning to improve the parameters systematically.

6.3 Classification Performance

We benchmark the accuracy of our methods against other methods based on Micro-F1, Macro-F1, Weighted-F1, Binary-F1, AUC-P and AUC-L scores. AUC-L is the AUC score evaluated on the binary predictions from the logistic classifier, whereas AUC-P is evaluated on the prediction probabilities. Contrary to AUC and Macro-F1, Micro-F1 and Binary-F1 do not consider class imbalance. As the datasets are all strongly unbalanced, as seen in Table 1, good scores for Micro and Binary-F1 can be achieved with classifiers that would always predict a positive sign.

The results are reported in Table 2. We reproduce the results of other methods from [Li et al., 2023]. All methods, including ours, use an embedding dimension of $k = 64$ and a training split of 80%. The parameters used for the test results on all datasets except BitcoinAlpha were trained on BitcoinAlpha. For the test on BitcoinAlpha, we have trained our models on BitcoinOTC, showing the generalizability of our method. This highlights how training can be done on a dataset different from the one the embedding generation is computed on. Although, SLGNN consistently obtains the best result, our methods SPR and SPR-NN fit into the scoreboard of the compared methods. In particular, SPR-NN often ranks second and obtains results very close to SDGNN.

Table 2: Link sign prediction results (mean±std). Results for all methods except SPR and SPR-NN are reproduced from [Li et al., 2023]. The best are bolded and second best underlined.

	Metrics	SIGNET	SGCN	SiGAT	SNEA	SGDNET	SDGNN	SLGNN	SPR	SPR-NN
Bit. Alpha	F1-MI	92.82±0.31	92.65±0.30	92.08±0.24	92.99±0.29	92.30±0.22	92.55±0.32	94.28 ±0.51	91.62 ±0.33	90.99 ±0.33
	F1-MA	74.91±1.33	75.67±1.46	72.93±0.92	76.46±1.19	75.22±0.92	78.04±1.03	83.61 ±0.94	73.0 ±1.39	76.10 ±0.95
	F1-WT	91.92±0.40	91.98±0.41	91.20±0.27	92.29±0.36	91.72±0.25	92.36±0.34	94.22 ±0.42	91.05±0.40	91.24±0.39
	F1-BI	96.11±0.17	95.99±0.16	95.70±0.13	96.19±0.16	95.79±0.12	95.89±0.17	96.83 ±0.29	95.42±0.18	95.07±0.19
	AUC-P	92.02±0.56	92.31±0.82	87.71±0.78	92.70±0.58	89.41±0.34	91.88±0.52	95.08 ±0.34	85.03±1.15	89.35±0.10
	AUC-L	70.29±1.26	71.99±1.74	69.05±0.97	72.31±1.20	72.14±1.25	76.75±1.21	82.88 ±0.82	70.4±1.54	76.67±0.14
Bit. OTC	F1-MI	90.68±0.29	91.72±0.25	90.54±0.26	92.28±0.27	91.80±0.47	92.26±0.28	94.48 ±0.33	90.85±0.23	91.97±0.43
	F1-MA	79.62±0.71	82.37±0.57	79.11±0.87	83.45±0.66	83.54±0.90	84.57±0.65	88.99 ±0.56	80.86±0.75	84.12±0.87
	F1-WT	90.09±0.33	91.32±0.27	89.88±0.35	91.87±0.30	91.67±0.46	92.16±0.31	94.41 ±0.31	90.46±0.23	91.95±0.41
	F1-BI	94.63±0.16	95.21±0.14	94.56±0.13	95.54±0.15	95.20±0.28	95.47±0.16	96.77 ±0.20	94.69±0.12	95.28±0.25
	AUC-P	90.78±0.73	92.31±0.28	94.70±0.58	93.84±0.52	92.97±0.67	94.19±0.26	96.87 ±0.39	89.18±0.54	92.61±0.56
	AUC-L	76.50±0.77	79.67±1.63	75.85±1.12	80.14±1.20	82.49±0.87	83.73±0.89	87.95 ±0.27	78.54±0.71s	84.0±0.73
Slashdot	F1-MI	83.28±0.10	83.17±0.17	82.93±0.08	84.74±1.00	84.22±0.12	84.05±1.08	87.83 ±0.09	83.80±0.09	85.33±0.16
	F1-MA	76.22±0.15	75.73±0.38	75.73±0.11	78.45±0.12	77.31±0.32	77.98±0.26	83.27 ±0.13	72.85±0.25	78.88±0.33
	F1-WT	82.65±0.11	82.40±0.23	82.29±0.08	84.23±0.09	83.53±0.18	83.72±0.19	87.61 ±0.10	82.31±0.15	85.26±0.19
	F1-BI	89.18±0.07	89.17±0.10	88.95±0.06	90.09±0.07	89.82±0.06	89.54±0.12	92.01 ±0.06	90.90±0.05	90.55±0.09
	AUC-P	84.42±0.08	87.75±0.30	89.35±0.10	90.00±0.10	88.98±0.15	88.59±0.11	93.22 ±0.05	86.80±0.08	88.90±0.26
	AUC-L	74.62±1.13	73.89±0.44	74.17±0.12	76.87±0.11	75.43±0.46	76.95±0.27	82.15 ±0.16	70.30±0.05	78.63±0.45
Epinions	F1-MI	91.25±0.05	92.34±0.05	90.75±0.06	92.48±0.05	91.76±0.44	92.71±0.40	94.40 ±0.08	90.49±0.12	91.33±0.13
	F1-MA	82.29±0.09	85.12±0.05	81.74±0.17	85.42±0.08	83.93±0.48	86.02±0.09	89.44 ±0.18	82.04±0.08	83.38±0.65
	F1-WT	90.71±0.05	92.04±0.05	90.31±0.06	92.20±0.05	91.43±0.06	92.48±0.05	94.28 ±0.09	90.16±0.08	90.79±0.23
	F1-BI	94.89±0.03	95.48±0.07	94.56±0.04	95.56±0.03	95.14±0.03	95.69±0.02	96.68 ±0.04	94.36±0.05	94.88±0.08
	AUC-P	93.19±0.06	95.17±0.03	94.35±0.05	95.30±0.07	94.42±0.06	95.06±0.06	97.02 ±0.06	93.38±0.08	92.68±1.15
	AUC-L	78.99±0.08	82.75±0.09	79.16±0.28	83.08±0.09	81.54±0.32	84.00±0.15	87.79 ±0.36	80.06±0.17	80.97±1.33

6.4 Runtime

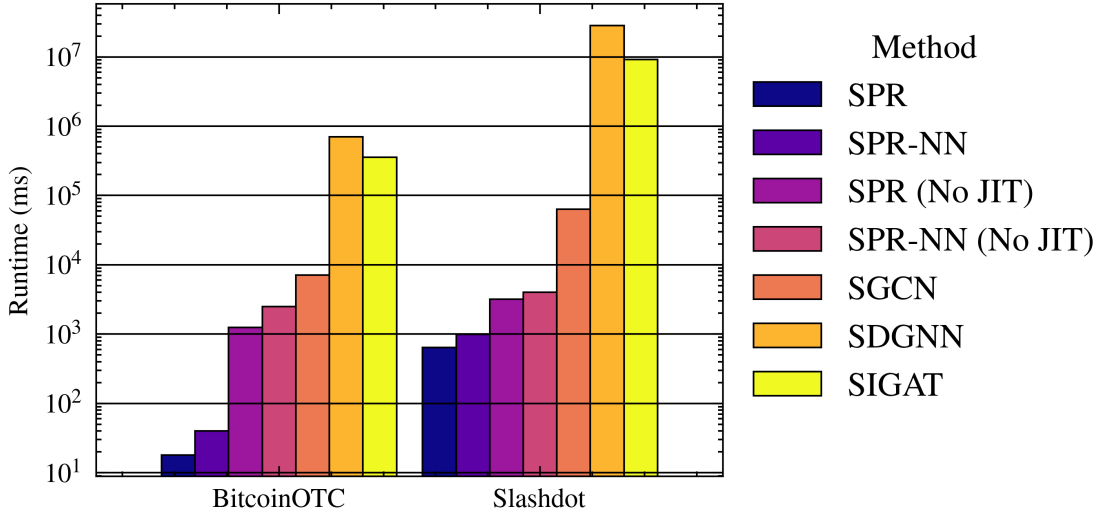


Figure 3: Runtime comparisons between different methods and datasets. Measurements are an average of over seven executions. Lower is better.

The embedding generation time of SPR and SPR-NN are measured and compared with SGCN [Derr et al., 2018], SiGAT [Huang et al., 2019] and SDGNN [Huang et al., 2021], where we rely on default settings of the reference implementations. We were not able to access the code for SLGNN. All methods are run on a system with the following specifications: AMD EPYC 7702 64-Core Processor: 16GB CPU RAM, NVIDIA Tesla T4: 80Gb GPU RAM, Ubuntu 20.04. Our methods are implemented using Python version 3.12.4, JAX version 0.4.31 and the Adam optimization method is from Optax 0.2.3.

All compared implementations SGCN, SiGAT, and SDGNN use Pytorch, while our methods use JAX. JAX and Pytorch are fully GPU-accelerated array computation libraries with just-in-time compilation (JIT) features, providing near-optimal performance [Bradbury et al., 2018, Ansel et al., 2024]. We measure only the node embedding generation time; graph processing computation of node and edge level features are excluded. In the case of SPR and SPR-NN node embedding generation time is equivalent to the duration it takes to solve the ODEs. For other methods, this means learning the parameters of a Graph Neural Network capable of generating the embeddings for a specific dataset. We measure the execution times in milliseconds on BitcoinOTC and Slashdot, representing a medium and large dataset. The graph sizes can be found in Table 1 and the results are shown in Figure 3. Due to the potential differing performance in

JIT capabilities of PyTorch and JAX, we include measurements where the JIT feature of JAX is disabled. In the case of BitcoinOTC, JIT drastically increases performance, an effect which is less prevalent in the case of Slashdot. JIT likely removes additional overhead, which is dominant in the case of the relatively small graph BitcoinAlpha but not so on Slashdot. The JIT compiled SPR-NN has a speedup factor of 63 over SGCN on the Slashdot dataset. Compared to the implementation of SDGNN, the speedup is 28654. Compared to SGCN, which has a similar accuracy performance to SPR and SPR-NN, the runtime performance improvements likely stem from the following sources:

- Better performance of the GSN layer compared to the GCN layer. This effect, however, is mostly hidden by GPU parallelization, as the layer operations can be executed in parallel.
- SPR and SPR-NN use only a single layer, whereas SGCN uses 32 consecutive layers. As the computation of the layers is serial, it cannot be parallelized.
- SGCN trains over 100 epochs, similarly to our methods, which use 120 Euler integration steps. The training process of SGCN, however, relies on backpropagation, which doubles its runtime compared to ours [Blakely et al., 2021].

7 Conclusion

In this paper, we investigate node feature vector generation for signed networks to optimize link sign prediction with a logistic classifier based on node vector distances. We propose an efficient message passing layer architecture called Graph Spring Network (GSN), which we combine with the Graph Neural ODE formalism. Based on this framework, we then propose the SPR method, which closely resembles the physical model of a spring, where each edge represents a spring that can store or release energy, generating node displacement. We extend the idea by replacing the spring mechanics with small artificial neural networks in SPR-NN. We train the specific dynamics of the ODEs for SPR and SPR-NN on a single dataset, allowing us to generate the node embeddings on novel datasets only by solving the ODEs using the Euler methods. We then perform experiments on four real-world signed networks and show that our proposed method SPR-NN performs similarly to other state-of-the-art feature vector generation methods in terms of accuracy. Furthermore, our method is significantly faster in embedding generation than the compared methods. Compared to other methods, our method marks the edges one wants to infer as neutral during embedding generation. When the sign of a new set of edges is asked, the embedding has to be regenerated, which is not necessarily the case in other methods. However, as our method is several orders of magnitude faster, regenerating the embeddings is not a problem. In further work SPR and SPR-NN could be adapted for directed networks and SPR-NN could be trained on more node features. Finally, the Graph Spring Network Layer (GSN) could be used for other node embedding generation tasks.

References

- Jure Leskovec, Daniel Huttenlocher, and Jon Kleinberg. Signed networks in social media. In *Proceedings of the SIGCHI Conference on Human Factors in Computing Systems*, pages 1361–1370, 2010.
- Junjie Huang, Ruobing Xie, Qi Cao, Huawei Shen, Shaoliang Zhang, Feng Xia, and Xueqi Cheng. Negative can be positive: Signed graph neural networks for recommendation. *Information Processing & Management*, 60(4):103403, 2023.
- Dorwin Cartwright and Frank Harary. Structural balance: a generalization of heider’s theory. *Psychological Review*, 63(5):277, 1956.
- Junjie Huang, Huawei Shen, Liang Hou, and Xueqi Cheng. Sdgnn: Learning node representation for signed directed networks. In *Proceedings of the AAAI Conference on Artificial Intelligence*, volume 35, pages 196–203, 2021.
- Tyler Derr, Yao Ma, and Jiliang Tang. Signed graph convolutional networks. In *2018 IEEE International Conference on Data Mining (ICDM)*, pages 929–934. IEEE, 2018.
- Michael Poli, Stefano Massaroli, Junyoung Park, Atsushi Yamashita, Hajime Asama, and Jinkyoo Park. Graph neural ordinary differential equations, 2019. Preprint at <https://arxiv.org/abs/1911.07532>.
- T Konstantin Rusch, Ben Chamberlain, James Rowbottom, Siddhartha Mishra, and Michael Bronstein. Graph-coupled oscillator networks. In *International Conference on Machine Learning*, pages 18888–18909. PMLR, 2022.
- Haiting Sun, Peng Tian, Yun Xiong, Yao Zhang, Yali Xiang, Xing Jia, and Haofen Wang. Dynamise: dynamic signed network embedding for link prediction. *Machine Learning*, 113(7):4037–4053, 2024.
- Haoxin Liu. Lightsgcn: Powering signed graph convolution network for link sign prediction with simplified architecture design. In *Proceedings of the 45th International ACM SIGIR Conference on Research and Development in Information Retrieval*, pages 2680–2685, 2022.

- Yu Li, Yuan Tian, Jiawei Zhang, and Yi Chang. Learning signed network embedding via graph attention. In *Proceedings of the AAAI conference on Artificial Intelligence*, volume 34, pages 4772–4779, 2020.
- Mohammad Raihanul Islam, B Aditya Prakash, and Naren Ramakrishnan. Signet: Scalable embeddings for signed networks. In *Advances in Knowledge Discovery and Data Mining: 22nd Pacific-Asia Conference, PAKDD 2018, Melbourne, VIC, Australia, June 3-6, 2018, Proceedings, Part II* 22, pages 157–169. Springer, 2018.
- Guojing Ren, Xiao Ding, Xiao-Ke Xu, and Hai-Feng Zhang. Link prediction in multilayer networks via cross-network embedding. In *Proceedings of the AAAI Conference on Artificial Intelligence*, volume 38, pages 8939–8947, 2024.
- Chanyoung Chung and Joyce Jiyoun Whang. Learning representations of bi-level knowledge graphs for reasoning beyond link prediction. In *Proceedings of the AAAI Conference on Artificial Intelligence*, volume 37, pages 4208–4216, 2023.
- Ramanathan Guha, Ravi Kumar, Prabhakar Raghavan, and Andrew Tomkins. Propagation of trust and distrust. In *Proceedings of the 13th international conference on World Wide Web*, pages 403–412, 2004.
- Dongjin Song and David A Meyer. Link sign prediction and ranking in signed directed social networks. *Social Network Analysis and Mining*, 5:1–14, 2015.
- Jure Leskovec, Kevin J Lang, Anirban Dasgupta, and Michael W Mahoney. Community structure in large networks: Natural cluster sizes and the absence of large well-defined clusters. *Internet Mathematics*, 6(1):29–123, 2009.
- Bryan Perozzi, Rami Al-Rfou, and Steven Skiena. Deepwalk: Online learning of social representations. In *Proceedings of the 20th ACM SIGKDD International Conference on Knowledge Discovery and Data Mining*, pages 701–710, 2014.
- Aditya Grover and Jure Leskovec. node2vec: Scalable feature learning for networks. In *Proceedings of the 22nd ACM SIGKDD International Conference on Knowledge Discovery and Data Mining*, pages 855–864, 2016.
- Lei Shi, Bin Hu, Deng Zhao, Jianshan He, Zhiqiang Zhang, and Jun Zhou. Structural information enhanced graph representation for link prediction. In *Proceedings of the AAAI Conference on Artificial Intelligence*, volume 38, pages 14964–14972, 2024.
- Suhang Wang, Jiliang Tang, Charu Aggarwal, Yi Chang, and Huan Liu. Signed network embedding in social media. In *Proceedings of the 2017 SIAM International Conference on Data Mining*, pages 327–335. SIAM, 2017.
- Yiqi Chen, Tiejun Qian, Huan Liu, and Ke Sun. "bridge" enhanced signed directed network embedding. In *Proceedings of the 27th ACM International Conference on Information and Knowledge Management*, pages 773–782, 2018a.
- Zhihong Fang, Shaolin Tan, and Yaonan Wang. A signed subgraph encoding approach via linear optimization for link sign prediction. *IEEE Transactions on Neural Networks and Learning Systems*, 2023.
- Petar Veličković, Guillem Cucurull, Arantxa Casanova, Adriana Romero, Pietro Lio, and Yoshua Bengio. Graph attention networks, 2017. Preprint at <https://arxiv.org/abs/1710.10903>.
- Junjie Huang, Huawei Shen, Liang Hou, and Xueqi Cheng. Signed graph attention networks. In *Artificial Neural Networks and Machine Learning—ICANN 2019: Workshop and Special Sessions: 28th International Conference on Artificial Neural Networks, Munich, Germany, September 17–19, 2019, Proceedings* 28, pages 566–577. Springer, 2019.
- Yu Li, Meng Qu, Jian Tang, and Yi Chang. Signed laplacian graph neural networks. In *Proceedings of the AAAI conference on Artificial Intelligence*, volume 37, pages 4444–4452, 2023.
- Tomasz Lizurej, Tomasz Michalak, and Stefan Dziembowski. On manipulating weight predictions in signed weighted networks. In *Proceedings of the AAAI Conference on Artificial Intelligence*, volume 37, pages 5222–5229, 2023.
- Dongjin Lee, Juho Lee, and Kijung Shin. Spear and shield: Adversarial attacks and defense methods for model-based link prediction on continuous-time dynamic graphs. In *Proceedings of the AAAI Conference on Artificial Intelligence*, volume 38, pages 13374–13382, 2024.
- Louis-Pascal Xhonneux, Meng Qu, and Jian Tang. Continuous graph neural networks. In *International Conference on Machine Learning*, pages 10432–10441. PMLR, 2020.
- Ricky TQ Chen, Yulia Rubanova, Jesse Bettencourt, and David K Duvenaud. Neural ordinary differential equations. In *Advances in Neural Information Processing Systems*, volume 31, 2018b.
- Zijie Huang, Yizhou Sun, and Wei Wang. Learning continuous system dynamics from irregularly-sampled partial observations. In *Advances in Neural Information Processing Systems*, volume 33, pages 16177–16187, 2020.
- Alvaro Sanchez-Gonzalez, Victor Bapst, Kyle Cranmer, and Peter Battaglia. Hamiltonian graph networks with ode integrators, 2019. Preprint at <https://arxiv.org/abs/1909.12790>.

- Qiyu Kang, Kai Zhao, Yang Song, Sijie Wang, and Wee Peng Tay. Node embedding from neural hamiltonian orbits in graph neural networks. In *International Conference on Machine Learning*, pages 15786–15808. PMLR, 2023.
- Ben Chamberlain, James Rowbottom, Maria I Gorinova, Michael Bronstein, Stefan Webb, and Emanuele Rossi. Grand: Graph neural diffusion. In *International Conference on Machine Learning*, pages 1407–1418. PMLR, 2021.
- Jinhong Jung, Jaemin Yoo, and U Kang. Signed graph diffusion network, 2020. Preprint at <https://arxiv.org/abs/2012.14191>.
- Jeongwhan Choi, Seoyoung Hong, Noseong Park, and Sung-Bae Cho. Gread: Graph neural reaction-diffusion networks. In *International Conference on Machine Learning*, pages 5722–5747. PMLR, 2023.
- Thomas MJ Fruchterman and Edward M Reingold. Graph drawing by force-directed placement. *Software: Practice and Experience*, 21(11):1129–1164, 1991.
- Tomihisa Kamada, Satoru Kawai, et al. An algorithm for drawing general undirected graphs. *Information Processing Letters*, 31(1):7–15, 1989.
- Ronny Hadany and David Harel. A multi-scale algorithm for drawing graphs nicely. *Discrete Applied Mathematics*, 113(1):3–21, 2001.
- Md Khaledur Rahman, Majedul Haque Sujon, and Ariful Azad. Force2vec: Parallel force-directed graph embedding. In *2020 IEEE International Conference on Data Mining (ICDM)*, pages 442–451. IEEE, 2020.
- Hamidreza Lotfalizadeh and Mohammad Al Hasan. Force-directed graph embedding with hops distance. In *2023 IEEE International Conference on Big Data (BigData)*, pages 2946–2953. IEEE, 2023.
- Michael M Bronstein, Joan Bruna, Taco Cohen, and Petar Veličković. Geometric deep learning: Grids, groups, graphs, geodesics, and gauges, 2021. Preprint available at <https://arxiv.org/abs/2104.13478>.
- Derrick Blakely, Jack Lanchantin, and Yanjun Qi. Time and space complexity of graph convolutional networks, 2021. Accessed: Dec. 13, 2024. [Online]. Available: https://qdata.github.io/deep2Read//talks-mb2019/Derrick_201906_GCN_complexityAnalysis-writeup.pdf.
- James Bradbury, Roy Frostig, Peter Hawkins, Matthew James Johnson, Chris Leary, Dougal Maclaurin, George Necula, Adam Paszke, Jake VanderPlas, Skye Wanderman-Milne, and Qiao Zhang. JAX: composable transformations of Python+NumPy programs, 2018. URL <http://github.com/google/jax>.
- Nils Thuerey, Philipp Holl, Maximilian Mueller, Patrick Schnell, Felix Trost, and Kiwon Um. Physics-based deep learning, 2021. Preprint at <https://arxiv.org/abs/2109.05237>.
- Jingzhao Zhang, Tianxing He, Suvrit Sra, and Ali Jadbabaie. Why gradient clipping accelerates training: A theoretical justification for adaptivity, 2019. Preprint at <https://arxiv.org/abs/1905.11881>.
- Diederik P Kingma and Jimmy Ba. Adam: A method for stochastic optimization, 2014. Preprint at <https://arxiv.org/abs/1412.6980>.
- Srijan Kumar, Francesca Spezzano, VS Subrahmanian, and Christos Faloutsos. Edge weight prediction in weighted signed networks. In *2016 IEEE 16th International Conference on Data Mining (ICDM)*, pages 221–230. IEEE, 2016.
- Matthew Richardson, Rakesh Agrawal, and Pedro Domingos. Trust management for the semantic web. In *International Semantic Web Conference*, pages 351–368. Springer, 2003.
- Jason Ansel, Edward Yang, Horace He, Natalia Gimelshein, Animesh Jain, Michael Voznesensky, Bin Bao, Peter Bell, David Berard, Evgeni Burovski, et al. Pytorch 2: Faster machine learning through dynamic python bytecode transformation and graph compilation. In *Proceedings of the 29th ACM International Conference on Architectural Support for Programming Languages and Operating Systems, Volume 2*, pages 929–947, 2024.